PRAMANA
— journal of
physics

Vol. 81, No. 4
October 2013
pp. 641–665

Convectively driven flow past an infinite moving vertical cylinder with thermal and mass stratification

RUDRA KANTA DEKA[1] and ASHISH PAUL[2,*]

[1]Department of Mathematics, Gauhati University, Guwahati 781 014, India
[2]Department of Mathematical Sciences, Bodoland University, Kokrajhar 783 370, India
*Corresponding author. E-mail: ashpaul85@gmail.com

MS received 13 November 2012; revised 14 June 2013; accepted 18 July 2013
DOI: 10.1007/s12043-013-0604-6; ***e*Publication:** 1 October 2013

Abstract. An analysis is performed to study the unsteady, incompressible, one-dimensional, free convective flow over an infinite moving vertical cylinder under combined buoyancy effects of heat and mass transfer with thermal and mass stratifications. Laplace transform technique is adopted for finding solutions for velocity, temperature and concentration with unit Prandtl and Schmidt numbers. Solutions of unsteady state for larger times are compared with the solutions of steady state. Velocity, temperature and concentration profiles are analysed for various sets of physical parameters. Skin friction, Nusselt number and Sherwood number are shown graphically. It has been found that the thermal as well as mass stratification affects the flow appreciably.

Keywords. Free convection; thermal stratification; mass stratification; Laplace transformation; vertical cylinder.

PACS Nos 67.10.Jn; 67.25.bd; 44.25.+f; 47.55.pb

1. Introduction

Unsteady, natural convection flow of a viscous incompressible fluid over a moving vertical cylinder with combined effects of heat and mass transfer is an important problem prevalent in many engineering and geophysical applications. These types of problems find application in nuclear reactor cooling system, underground energy transport system and oceanography.

Sparrow and Gregg [1] first studied the heat transfer from vertical cylinders. Subsequently, Goldstein and Briggs [2] presented an analytical study of the transient, free convective flow past a vertical plate and a circular cylinder by employing Laplace transform technique. Bottemanne [3] studied the combined effect of heat and mass transfer in the steady laminar boundary layer of a vertical cylinder placed in still air. Chen and

Yuh [4] studied steady heat and mass transfer processes near the cylinders. Their study covered a wide range of radii and Prandtl numbers. Heckel *et al* [5] studied the steady, free convection along a slender vertical cylinder with variable surface temperature and presented the results for various Prandtl numbers of 0.1, 0.7, 7 and 100. Gorla [6] presented a numerical solution of steady, combined, free and forced convection in the boundary layer flow of a micropolar fluid past a continuous moving vertical cylinder. Velusamy and Garg [7] studied natural convection adjacent to a heat generating vertical cylinder. Ganesan and Rani [8] presented a numerical solution for the transient natural convection flow over a vertical cylinder under the combined buoyancy effects of heat and mass transfer. Thereafter, Ganesan and Loganathan [9–11] presented a numerical analysis of unsteady natural convective flow past a semi-infinite vertical cylinder with heat and mass transfer under different physical situations. Rani [12] presented a numerical study on transient natural convection along a vertical cylinder with variable surface temperature and mass diffusion. In all these studies, thermal and mass stratifications are not taken into account.

Shapiro and Fedorovish [13] presented analytical solution of one-dimensional laminar natural convection along an infinite vertical plate by introducing the pressure work term and the ambient thermal stratification in the thermodynamic energy equation for Prandtl number of unity. They found that stratification provides a negative feedback mechanism: warm fluid rises, expands and cools relative to the environment, whereas cool fluid subsides, compresses and warms relative to the environment. Loganathan and Ganesan [14] presented a numerical study of free convective flow of a viscous incompressible fluid past a moving, semi-infinite, vertical cylinder with constant temperature and mass diffusion in a thermally stratified medium by employing an implicit finite-difference scheme of Crank–Nicolson type. Takhar *et al* [16] obtained numerical solutions by finite-difference scheme for a flow past a continuously moving vertical surface immersed in a stratified fluid. Cheng [15] studied the coupled heat and mass transfer effects near a vertical wavy surface in a non-Newtonian fluid-saturated porous medium in the presence of thermal and mass stratifications and obtained solutions by collocation method. Recently, Deka and Paul [17,18] presented an analytical study of the transient-free convection flow past an infinite vertical cylinder in a stably stratified fluid by employing the Laplace transform technique.

Many researchers have shown interest in the study of transient natural convective flow past vertical cylinder under various physical situations. However, analytical approach for the combined effects of thermal and mass stratifications has not been considered for a moving vertical cylinder, which is necessary for validating numerical models. The simultaneous effects of thermal and mass stratifications have application in meteorology and oceanography. In this work, attempt has been made to present an analytical investigation of one-dimensional free convective flow past an infinite moving vertical cylinder in the presence of thermal and mass stratifications. The unsteady non-dimensional linear governing equations are solved by the Laplace transform technique for unit Prandtl number and unit Schmidt number. The solutions thus obtained for the fluid with the two stratifications are compared with the classical solutions, i.e. solutions corresponding to the fluid without thermal and mass stratifications. Also, solutions of unsteady state for larger times are compared with the solutions of steady state.

2. Mathematical analysis

Consider an unsteady, laminar and incompressible viscous flow past an infinite moving vertical cylinder of radius r_0. Here, the x'-axis is taken vertically upward along the axis of the cylinder and the radial coordinate r' is taken normal to the cylinder. The ensuing motion is one-dimensional with the non-zero vertical component of velocity u', varying only in the x'-direction. Accordingly, the equation of continuity is trivially satisfied. The physical model of the problem and the coordinate system are shown in figure 1. We decompose the fluid temperature and concentration into its environmental and perturbation components, $T(x', r', t') = T'_\infty(x') + T'(r', t')$, $C(x', r', t') = C'_\infty(x') + C'(r', t')$, so that the one-dimensional flow behaviour is well defined. It is assumed that at time $t' > 0$, the cylinder starts to move in the vertical direction with constant velocity u_0. Also, constant perturbation temperature (T_0) and concentration (C_0) are specified near the surface of the cylinder. Then, following Boussinesq's approximation, the one-dimensional equations for momentum, energy and concentration are as follows:

$$\frac{\partial u'}{\partial t'} = \frac{\nu}{r'}\frac{\partial}{\partial r'}\left(r'\frac{\partial u'}{\partial r'}\right) + g\beta T' + g\beta^* C', \tag{1}$$

$$\frac{\partial T'}{\partial t'} = \frac{\alpha}{r'}\frac{\partial}{\partial r'}\left(r'\frac{\partial T'}{\partial r'}\right) - \gamma u', \tag{2}$$

$$\frac{\partial C'}{\partial t'} = \frac{D}{r'}\frac{\partial}{\partial r'}\left(r'\frac{\partial C'}{\partial r'}\right) - \xi u'. \tag{3}$$

Here ν is the kinematic viscosity, g is the acceleration due to gravity, β is the volumetric coefficient of thermal expansion, β* is the volumetric coefficient of expansion with concentration, α is the thermal diffusivity of fluid, γ is the thermal stratification parameter, D is the mass diffusion coefficient and ξ is the mass stratification parameter.

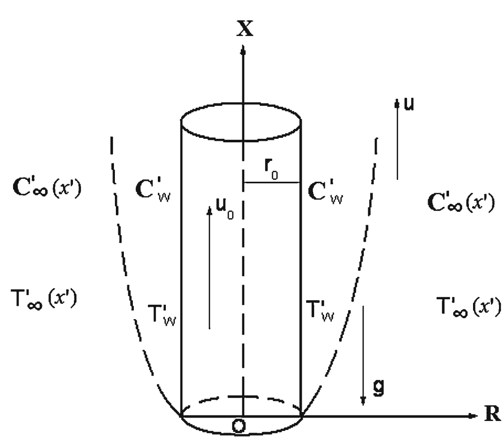

Figure 1. The physical model and coordinate system.

The initial and boundary conditions for velocity, perturbation temperature and concentration are,

$$\left.\begin{array}{ll} t' \le 0: & u' = 0, \quad T' = 0, \quad C' = 0 \qquad \forall\, r' \\ t > 0: & u' = u_0, \;\; T' = T_0, \;\; C' = C_0 \;\; \text{at} \;\; r' = r_0 \\ & u' \to 0, \;\; T' \to 0, \;\; C' \to 0 \;\; \text{as} \;\; r' \to \infty \end{array}\right\}. \tag{4}$$

However, the thermal stratification parameter $\gamma = \mathrm{d}T'_\infty(x')/\mathrm{d}x' + g/C_p$, is the main concern in our study. The thermal stratification is the combination of the vertical temperature advection $(= \mathrm{d}T'_\infty(x')/\mathrm{d}x')$, where the ambient fluid temperature depends on the height and the work of compression $(= g/C_p)$, the rate of reversible work done on the fluid particles by compression. In an adiabatic environment, $\mathrm{d}T'_\infty(x')/\mathrm{d}x' + g/C_p = 0$. In that case $\mathrm{d}T'_\infty(x')/\mathrm{d}x' = -g/C_p$ and $(-g/C_p)$ is called the adiabatic temperature gradient and is the largest rate at which the temperature can decrease with height without causing instability. The stability of the atmosphere is determined according to $\gamma > 0$ (stable), $\gamma = 0$ (neutral), $\gamma < 0$ (unstable). For the air at normal temperature and pressure, the temperature of neutral atmosphere decreases with height at the rate of $g/C_p \cong 10°\text{C/km}$. Meteorologists termed vertical temperature gradients as 'lapse rate', so that in their terminology the adiabatic lapse rate is 10°C/km. A similar variable $\xi = \mathrm{d}C'_\infty(x')/\mathrm{d}x'$, is termed as mass stratification parameter. In the context of oceanography, mass stratification exists due to the salinity of sea water. The work of compression, though small (since $g = 9.8$ m s^{-2} and at 20°C, $C_p = 4182$ J kg^{-1} K^{-1} for water, while for dry air $C_p = 1012$ J kg^{-1} K^{-1} (see Kundu [19])), may play an important role combined with vertical temperature advection.

Introducing the non-dimensional quantities,

$$\left.\begin{array}{l} R = \dfrac{r}{r_0}, \quad U = \dfrac{u}{u_0}, \quad t = \dfrac{t'\nu}{r_0^2}, \quad \theta = \dfrac{T'}{T_0}, \quad \phi = \dfrac{C'}{C_0}, \quad \mathrm{Pr} = \dfrac{\nu}{\alpha}, \quad \mathrm{Sc} = \dfrac{\nu}{\mathrm{D}} \\ \mathrm{Gr} = \mathrm{g}\beta\, \mathrm{r}_0^2 \dfrac{\mathrm{T}_0}{\mathrm{u}_0\nu}, \quad \mathrm{Gc} = g\beta^* r_0^2 \dfrac{C_0}{u_0\nu}, \quad S = \dfrac{\gamma u_0 r_0^2}{\nu T_0}, \quad F = \dfrac{\xi u_0 r_0^2}{\nu C_0} \end{array}\right\} \tag{5}$$

the equations (1)–(3) reduce to

$$\frac{\partial U}{\partial t} = \frac{\partial^2 U}{\partial R^2} + \frac{1}{R}\frac{\partial U}{\partial R} + \mathrm{Gr}\,\theta + \mathrm{Gc}\,\phi \tag{6}$$

$$\frac{\partial \theta}{\partial t} = \frac{1}{\mathrm{Pr}}\left(\frac{\partial^2 \theta}{\partial R^2} + \frac{1}{R}\frac{\partial \theta}{\partial R}\right) - SU \tag{7}$$

$$\frac{\partial \phi}{\partial t} = \frac{1}{\mathrm{Sc}}\left(\frac{\partial^2 \phi}{\partial R^2} + \frac{1}{R}\frac{\partial \phi}{\partial R}\right) - FU \tag{8}$$

with the following initial and boundary conditions:

$$\left.\begin{array}{ll} t \le 0: & U = 0, \quad \theta = 0, \quad \phi = 0 \qquad \forall\, R \\ t > 0: & U = 1, \quad \theta = 1, \quad \phi = 1 \quad \text{at} \quad R = 1 \\ & U \to 0, \;\; \theta \to 0, \;\; \phi \to 0 \;\; \text{as} \;\; R \to \infty \end{array}\right\}. \tag{9}$$

Here U is the dimensionless velocity, Gr is the thermal Grashof number, Gc is the mass Grashof number, Pr is the Prandtl number, θ is the dimensionless temperature, R is the dimensionless radial distance, S is the dimensionless thermal stratification parameter.

Also, R is the dimensionless radial distance, ϕ is the dimensionless concentration, Sc is the Sherwood number, t is the dimensionless time and F is the dimensionless mass stratification parameter.

3. Solutions

To solve the governing non-dimensional unsteady equations (6)–(8) subject to initial and boundary conditions (9), we apply Laplace transform technique for the case of unit Prandtl number and Schmidt number, as for arbitrary Prandtl number or Schmidt number, the Laplace transform technique leads to an equation of non-tractable form. Thus, taking Laplace transforms of (6), (7) and (8) we get

$$\frac{\mathrm{d}^2\bar{U}}{\mathrm{d}R^2} + \frac{1}{R}\frac{\mathrm{d}\bar{U}}{\mathrm{d}R} - p\bar{U} + \mathrm{Gr}\,\bar{\theta} + \mathrm{Gc}\,\bar{\phi} = 0, \tag{10}$$

$$\frac{\mathrm{d}^2\bar{\theta}}{\mathrm{d}R^2} + \frac{1}{R}\frac{\mathrm{d}\bar{\theta}}{\mathrm{d}R} - p\bar{\theta} - S\bar{U} = 0, \tag{11}$$

$$\frac{\mathrm{d}^2\bar{\phi}}{\mathrm{d}R^2} + \frac{1}{R}\frac{\mathrm{d}\bar{\phi}}{\mathrm{d}R} - p\bar{\phi} - F\bar{U} = 0, \tag{12}$$

where p is the parameter of the Laplace transformation defined by, for example, $L\{\theta(R,t)\} = \int_0^\infty \mathrm{e}^{-pt}\theta(R,t)\mathrm{d}t = \bar{\theta}(R,p)$. Using eqs (11) and (12), we eliminate $\bar{\theta}$, $\bar{\phi}$ from (10) and after rearrangement, we have

$$\left\{\frac{\mathrm{d}^2}{\mathrm{d}R^2} + \frac{1}{R}\frac{\mathrm{d}}{\mathrm{d}R} - a^2\right\}\left\{\frac{\mathrm{d}^2}{\mathrm{d}R^2} + \frac{1}{R}\frac{\mathrm{d}}{\mathrm{d}R} - b^2\right\}\bar{U} = 0, \tag{13}$$

where

$$a^2 = p + iM, \quad b^2 = p - iM \quad \text{and} \quad M^2 = S\mathrm{Gr} + F\mathrm{Gc}.$$

Now, assuming

$$\left\{\frac{\mathrm{d}^2}{\mathrm{d}R^2} + \frac{1}{R}\frac{\mathrm{d}}{\mathrm{d}R} - b^2\right\}\bar{U} = W \tag{14}$$

we have from (13)

$$\left\{\frac{\mathrm{d}^2}{\mathrm{d}R^2} + \frac{1}{R}\frac{\mathrm{d}}{\mathrm{d}R} - a^2\right\} W = 0$$

giving the solution $W(R) = C_1 I_0(aR) + C_2 K_0(aR)$, where C_1 and C_2 are arbitrary constants. Using $W(R)$ in (14) and applying variation of parameter technique, we have the solution for $\bar{U}(R,p)$ as

$$\bar{U} = \frac{C_1 I_0(aR)}{2iM} + \frac{C_2 K_0(aR)}{2iM} + C_3 I_0(bR) + C_4 K_0(bR), \tag{15}$$

where C_3 and C_4 are constants of integration. Since, $I_0(aR)$ and $I_0(bR)$ are unbounded as $R \to \infty$, we set $C_1 = 0$ and $C_3 = 0$ and with this assumption we finally have,

$$\bar{U} = \frac{C_2 K_0(aR)}{2iM} + C_4 K_0(bR). \tag{16}$$

In determining $\bar{U}$, we have used the following properties on Bessel function (see Carslaw and Jaeger [20]), namely,

$$\frac{\mathrm{d}}{\mathrm{d}R} I_0(bR) = bI_1(bR), \qquad \frac{\mathrm{d}}{\mathrm{d}R} K_0(bR) = -bK_1(bR),$$

$$I_0(bR)K_1(bR) + I_1(bR)K_0(bR) = \frac{1}{bR}.$$

Also, the following identities are derived and used in the determination of $\bar{U}$, namely,

$$\int RI_0(aR)I_0(bR)\,\mathrm{d}R = \frac{R}{a^2-b^2}[aI_0(bR)I_1(aR) - bI_0(aR)I_1(bR)],$$

$$\int RI_0(aR)K_0(bR)\,\mathrm{d}R = \frac{R}{a^2-b^2}[aI_1(aR)K_0(bR) + bI_0(aR)K_1(bR)],$$

$$\int RK_0(aR)K_0(bR)\mathrm{d}R = \frac{R}{a^2-b^2}[bK_0(aR)K_1(bR) - aK_0(bR)K_1(aR)].$$

Now, using eq. (16) in eq. (10) and above properties and identities, we have

$$C_2 K_0(aR) - 2iMC_4K_0(bR) + 2\,\mathrm{Gr}\,\bar{\theta} + 2\,\mathrm{Gr}\,\bar{\phi} = 0. \tag{17}$$

To determine C_2 and C_4, we apply Laplace transformation to the conditions $U = \theta = \phi = 1$ and then using (16), (17) for $R = 1$, we obtain

$$C_2 = \frac{iM - (\mathrm{Gr}+\mathrm{Gc})}{pK_0\left(\sqrt{p+iM}\right)} \quad \text{and} \quad C_4 = \frac{iM + (\mathrm{Gr}+\mathrm{Gc})}{2iM\,pK_0\left(\sqrt{p-iM}\right)}.$$

Thus we have,

$$\bar{U} = \frac{1}{2}\left\{\frac{K_0\left(R\sqrt{p+iM}\right)}{pK_0\left(\sqrt{p+iM}\right)} + \frac{K_0\left(R\sqrt{p-iM}\right)}{pK_0\left(\sqrt{p-iM}\right)}\right\}$$
$$- \frac{\mathrm{Gr}+\mathrm{Gc}}{2iM}\left\{\frac{K_0\left(R\sqrt{p+iM}\right)}{pK_0\left(\sqrt{p+iM}\right)} - \frac{K_0\left(R\sqrt{p-iM}\right)}{pK_0\left(\sqrt{p-iM}\right)}\right\}. \tag{18}$$

It is to be noted that for arbitrary Prandtl number (Pr $\neq 1$) and Schmidt number (Sc $\neq 1$), the elimination of $\bar{\theta}$, $\bar{\phi}$ leads to an equation of sixth order in $\bar{U}$ and this equation is not found tractable for finding solution of $\bar{U}$ analytically.

Thereafter, we substitute $\bar{U}$ in (11), and using the same procedure we obtain the Laplace transform of θ, i.e. $\bar{\theta}$, as

$$\bar{\theta} = \frac{(F-S)\mathrm{Gc}}{M^2}\frac{K_0\left(R\sqrt{p}\right)}{pK_0\left(\sqrt{p}\right)} + \frac{S}{2iM}\left\{\frac{K_0\left(R\sqrt{p+iM}\right)}{pK_0\left(\sqrt{p+iM}\right)} - \frac{K_0\left(R\sqrt{p-iM}\right)}{pK_0\left(\sqrt{p-iM}\right)}\right\}$$

$$+ \frac{S(\mathrm{Gr}+\mathrm{Gc})}{2M^2}\left\{\frac{K_0\left(R\sqrt{p-iM}\right)}{pK_0\left(\sqrt{p-iM}\right)} + \frac{K_0\left(R\sqrt{p+iM}\right)}{pK_0\left(\sqrt{p+iM}\right)}\right\}. \tag{19}$$

Also, from the similar nature of eq. (12) with eq. (11), we find

$$\bar{\phi} = \frac{\mathrm{Gr}(S-F)}{M^2}\frac{K_0\left(R\sqrt{p}\right)}{pK_0\left(\sqrt{p}\right)}$$

$$+ \frac{F}{2iM}\left\{\frac{K_0\left(R\sqrt{p+iM}\right)}{pK_0\left(\sqrt{p+iM}\right)} - \frac{K_0\left(R\sqrt{p-iM}\right)}{pK_0\left(\sqrt{p-iM}\right)}\right\}$$

$$+ \frac{F(\mathrm{Gr}+\mathrm{Gc})}{2M^2}\left\{\frac{K_0\left(R\sqrt{p-iM}\right)}{pK_0\left(\sqrt{p-iM}\right)} + \frac{K_0\left(R\sqrt{p+iM}\right)}{pK_0\left(\sqrt{p+iM}\right)}\right\}. \tag{20}$$

Now, we apply Bromwich contour of integration to find the Laplace inverse of $\bar{U}$ for Pr $= 1$ as (the details of finding the inverse is explained in the Appendix),

$$U = \frac{1}{2}\left\{\frac{K_0\left(R\sqrt{-iM}\right)}{K_0(M)} + \frac{K_0\left(R\sqrt{iM}\right)}{K_0\left(\sqrt{iM}\right)}\right\}$$

$$+ \frac{\mathrm{Gr}+\mathrm{Gc}}{2Mi}\left\{\frac{K_0\left(R\sqrt{-iM}\right)}{K_0\left(\sqrt{-iM}\right)} - \frac{K_0\left(R\sqrt{iM}\right)}{K_0\left(\sqrt{iM}\right)}\right\}$$

$$+ \frac{2\,(\mathrm{Gr}+\mathrm{Gc})}{\pi M}\int_0^\infty \frac{\mathrm{e}^{-V^2 t}\left\{V^2\sin(Mt)+M\cos(Mt)\right\}}{V^4+M^2}\Gamma(R,V)\,V\mathrm{d}V$$

$$+ \frac{2}{\pi}\int_0^\infty \frac{\mathrm{e}^{-V^2 t}\left\{V^2\cos(Mt)-L\sin(Mt)\right\}}{V^4+M^2}\Gamma(R,V)\,V\mathrm{d}V. \tag{21}$$

Here K_0 is the modified Bessel function of the second kind and order zero. Also, K_1, I_0 and I_1 are the modified Bessel function of the second kind and order one, modified Bessel function of the first kind and order zero and modified Bessel functions of the first kind and order one respectively. Similarly, we obtain the inverse for $\bar{\theta}$ and $\bar{\phi}$ as,

$$\begin{aligned}\theta = {} & \frac{\mathrm{Gc}(F-S)}{M^2}\left\{1+\frac{2}{\pi}\int_0^{\infty} \mathrm{e}^{-V^2 t}\,\Gamma(R,V)\,\frac{\mathrm{d}V}{V}\right\} \\ & - \frac{S}{2iM}\left\{\frac{K_0\big(R\sqrt{-iM}\big)}{K_0\big(\sqrt{-iM}\big)} - \frac{K_0\big(R\sqrt{iM}\big)}{K_0\big(\sqrt{iM}\big)}\right\} \\ & + \frac{S(\mathrm{Gr}+\mathrm{Gc})}{2M^2}\left\{\frac{K_0\big(R\sqrt{-iM}\big)}{K_0\big(\sqrt{-iM}\big)} + \frac{K_0\big(R\sqrt{iM}\big)}{K_0\big(\sqrt{iM}\big)}\right\} \\ & - \frac{2S}{\pi M}\int_0^{\infty}\frac{\mathrm{e}^{-V^2 t}\left\{V^2\sin(Mt)+M\cos(Mt)\right\}}{V^4+M^2}\Gamma(R,V)V\,\mathrm{d}V \\ & + \frac{2S(\mathrm{Gr}+\mathrm{Gc})}{\pi M^2}\int_0^{\infty}\frac{\mathrm{e}^{-V^2 t}\left\{V^2\cos(Mt)-M\sin(Mt)\right\}}{V^4+M^2}\Gamma(R,V)V\,\mathrm{d}V,\end{aligned} \tag{22}$$

$$\begin{aligned}\phi = {} & \frac{\mathrm{Gr}(S-F)}{M^2}\left\{1+\frac{2}{\pi}\int_0^{\infty} \mathrm{e}^{-V^2 t}\,\Gamma(R,V)\,\frac{\mathrm{d}V}{V}\right\} \\ & - \frac{F}{2iM}\left\{\frac{K_0\big(R\sqrt{-iM}\big)}{K_0\big(\sqrt{-iM}\big)} - \frac{K_0\big(R\sqrt{iM}\big)}{K_0\big(\sqrt{iM}\big)}\right\} \\ & + \frac{F(\mathrm{Gr}+\mathrm{Gc})}{2M^2}\left\{\frac{K_0\big(R\sqrt{-iM}\big)}{K_0\big(\sqrt{-iM}\big)} + \frac{K_0\big(R\sqrt{iM}\big)}{K_0\big(\sqrt{iM}\big)}\right\} \\ & - \frac{2F}{\pi M}\int_0^{\infty}\frac{\mathrm{e}^{-V^2 t}\left\{V^2\sin(Mt)+M\cos(Mt)\right\}}{V^4+M^2}\Gamma(R,V)V\,\mathrm{d}V \\ & + \frac{2F(\mathrm{Gr}+\mathrm{Gc})}{\pi M^2}\int_0^{\infty}\frac{\mathrm{e}^{-V^2 t}\left\{V^2\cos(Mt)-M\sin(Mt)\right\}}{V^4+M^2}\Gamma(R,V)V\,\mathrm{d}V.\end{aligned} \tag{23}$$

It is clearly seen that the expressions of θ and ϕ are identical only when the thermal stratification equals mass stratification ($S = F$). However, from the physical point of view it is not necessary that the thermal stratification should be equal to the mass stratification and hence the distinction between the expressions of θ and ϕ is retained.

The skin friction (shear stress on the surface) in non-dimensional form is given by

$$\tau = -\left.\frac{\partial U}{\partial R}\right|_{R=1}$$

and from eq. (21), it is derived as

$$\tau = \frac{1}{2}\left\{\frac{\sqrt{-iM}K_1\left(\sqrt{-iM}\right)}{K_0\left(\sqrt{-iM}\right)} + \frac{\sqrt{iM}K_1\left(\sqrt{iM}\right)}{K_0\left(\sqrt{iM}\right)}\right\}$$
$$+ \frac{\mathrm{Gr}+\mathrm{Gc}}{2Mi}\left\{\frac{\sqrt{-iM}K_1\left(\sqrt{-iM}\right)}{K_0\left(\sqrt{-iM}\right)} - \frac{\sqrt{iM}K_1\left(\sqrt{iM}\right)}{K_0\left(\sqrt{iM}\right)}\right\}$$
$$+ \frac{2}{\pi}\int_0^\infty \frac{\mathrm{e}^{-V^2t}\left\{V^2\cos(Mt) - M\sin(Mt)\right\}}{V^4+M^2}\Gamma_1(V)V^2\mathrm{d}V$$
$$+ \frac{2\,(\mathrm{Gr}+\mathrm{Gc})}{\pi M}\int_0^\infty \frac{\mathrm{e}^{-V^2t}\left\{V^2\sin(Mt) + M\cos(Mt)\right\}}{V^4+M^2}\Gamma_1(V)V^2\mathrm{d}V. \tag{24}$$

The rate of heat transfer (Nusselt number) in non-dimensional form is expressed as

$$\mathrm{Nu} = -\left.\frac{\partial\theta}{\partial R}\right|_{R=1}$$

and from eq. (22), it is derived as

$$\mathrm{Nu} = \frac{2\mathrm{Gc}(F-S)}{\pi M^2}\int_0^\infty \mathrm{e}^{-V^2t}\Gamma_1(V)\,\mathrm{d}V$$
$$- \frac{S}{2iM}\left\{\frac{\sqrt{-iM}K_1\left(\sqrt{-iM}\right)}{K_0\left(\sqrt{-iM}\right)} - \frac{\sqrt{iM}K_1\left(\sqrt{iM}\right)}{K_0\left(\sqrt{iM}\right)}\right\}$$
$$+ \frac{S(\mathrm{Gr}+\mathrm{Gc})}{2M^2}\left\{\frac{\sqrt{-iM}K_1\left(\sqrt{-iM}\right)}{K_0\left(\sqrt{-iM}\right)} + \frac{\sqrt{iM}K_1\left(\sqrt{iM}\right)}{K_0\left(\sqrt{iM}\right)}\right\}$$
$$- \frac{2S}{\pi M}\int_0^\infty \frac{\mathrm{e}^{-V^2t}\left\{V^2\sin(Mt) + M\cos(Mt)\right\}}{V^4+M^2}\Gamma_1(V)V^2\mathrm{d}V$$
$$+ \frac{2S(\mathrm{Gr}+\mathrm{Gc})}{\pi M^2}\int_0^\infty \frac{\mathrm{e}^{-V^2t}\left\{V^2\cos(Mt) - M\sin(Mt)\right\}}{V^4+M^2}\Gamma_1(V)V^2\mathrm{d}V. \tag{25}$$

The rate of mass transfer (Sherwood number) in non-dimensional form is given by

$$\mathrm{Sh} = -\left.\frac{\partial\phi}{\partial R}\right|_{R=1}$$

and from eq. (23), it is derived as

$$
\begin{aligned}
\mathrm{Sh} = {} & \frac{2\mathrm{Gr}(S-F)}{\pi M^2}\int_0^\infty \mathrm{e}^{-V^2 t}\Gamma_1(V)\,\mathrm{d}V \\
& - \frac{F}{2iM}\left\{\frac{\sqrt{-iM}K_1\big(\sqrt{-iM}\big)}{K_0\big(\sqrt{-iM}\big)} - \frac{\sqrt{iM}K_1\big(\sqrt{iM}\big)}{K_0\big(\sqrt{iM}\big)}\right\} \\
& + \frac{F(\mathrm{Gr}+\mathrm{Gc})}{2M^2}\left\{\frac{\sqrt{-iM}K_1\big(\sqrt{-iM}\big)}{K_0\big(\sqrt{-iM}\big)} + \frac{\sqrt{iM}K_1\big(\sqrt{iM}\big)}{K_0\big(\sqrt{iM}\big)}\right\} \\
& - \frac{2F}{\pi M}\int_0^\infty \frac{\mathrm{e}^{-V^2 t}\left\{V^2\sin(Mt) + M\cos(Mt)\right\}}{V^4+M^2}\Gamma_1(V)V^2\mathrm{d}V \\
& + \frac{2F(\mathrm{Gr}+\mathrm{Gc})}{\pi M^2}\int_0^\infty \frac{\mathrm{e}^{-V^2 t}\left\{V^2\cos(Mt) - M\sin(Mt)\right\}}{V^4+M^2}\Gamma_1(V)V^2\mathrm{d}V,
\end{aligned}
\tag{26}
$$

where

$$
\Gamma(R,V) = \frac{J_0(RV)Y_0(V) - Y_0(RV)J_0(V)}{J_0^2(V)+Y_0^2(V)}
$$

and

$$
\Gamma_1(V) = \frac{J_1(V)Y_0(V) - Y_1(V)J_0(V)}{J_0^2(V)+Y_0^2(V)}. \tag{27}
$$

Here, J_0 and Y_0 are respectively the Bessel function of the first kind and order zero and the Bessel function of the second kind and order zero. Also, J_1 and Y_1 are the Bessel functions of the first kind and order one and Bessel function of the second kind and order one respectively.

It is to be noted that in absence of mass transport ($\mathrm{Gc} = 0$), the present work coincides with the work of Deka and Paul [17]. Accordingly, the expressions for U, θ, τ and Nu given by eqs (21), (22), (24) and (25) revert to the expressions for velocity, temperature, skin friction and Nusselt number in Deka and Paul [17].

4. Steady-state solutions

Steady-state equations are obtained by neglecting the time derivative terms in eqs (6), (7) and (8). We solve these resulting ordinary differential equations subject to the boundary conditions (9) and obtain the expressions of steady-state velocity (U_s), temperature (θ_s) and concentration (ϕ_s) profiles as

$$
\begin{aligned}
U_\mathrm{s} = {} & \frac{1}{2}\left\{\frac{K_0\big(R\sqrt{-iM}\big)}{K_0\big(\sqrt{-iM}\big)} + \frac{K_0\big(R\sqrt{iM}\big)}{K_0\big(\sqrt{iM}\big)}\right\} \\
& + \frac{\mathrm{Gr}+\mathrm{Gc}}{2Mi}\left\{\frac{K_0\big(R\sqrt{-iM}\big)}{K_0\big(\sqrt{-iM}\big)} - \frac{K_0\big(R\sqrt{iM}\big)}{K_0\big(\sqrt{iM}\big)}\right\},
\end{aligned}
\tag{28}
$$

$$\theta_{\rm s} = \frac{{\rm Gc}(F-S)}{M^2} - \frac{S}{2iM}\left\{\frac{K_0\left(R\sqrt{-iM}\right)}{K_0\left(\sqrt{-iM}\right)} - \frac{K_0\left(R\sqrt{iM}\right)}{K_0\left(\sqrt{iM}\right)}\right\}$$

$$+ \frac{S({\rm Gr}+{\rm Gc})}{2M^2}\left\{\frac{K_0\left(R\sqrt{-iM}\right)}{K_0\left(\sqrt{-iM}\right)} + \frac{K_0\left(R\sqrt{iM}\right)}{K_0\left(\sqrt{iM}\right)}\right\}, \tag{29}$$

$$\phi_{\rm s} = \frac{{\rm Gr}(S-F)}{M^2} - \frac{F}{2iM}\left\{\frac{K_0\left(R\sqrt{-iM}\right)}{K_0\left(\sqrt{-iM}\right)} - \frac{K_0\left(R\sqrt{iM}\right)}{K_0\left(\sqrt{iM}\right)}\right\}$$

$$+ \frac{F({\rm Gr}+{\rm Gc})}{2M^2}\left\{\frac{K_0\left(R\sqrt{-iM}\right)}{K_0\left(\sqrt{-iM}\right)} + \frac{K_0\left(R\sqrt{iM}\right)}{K_0\left(\sqrt{iM}\right)}\right\}. \tag{30}$$

In non-dimensional form, the steady-state expressions of skin friction; $\tau_{\rm s} = -\left(\partial U_{\rm s}/\partial R\right)|_{R=1}$, Nusselt number; ${\rm Nu}_{\rm S} = -\left(\partial\theta_{\rm s}/\partial R\right)|_{R=1}$ and Sherwood Number; ${\rm Sh}_{\rm s} = -\left(\partial\phi_{\rm s}/\partial R\right)|_{R=1}$ are obtained from eqs (28), (29) and (30) respectively as

$$\tau_{\rm s} = \frac{1}{2}\left\{\frac{\sqrt{-iM}K_1\left(\sqrt{-iM}\right)}{K_0\left(\sqrt{-iM}\right)} + \frac{\sqrt{iM}K_1\left(\sqrt{iM}\right)}{K_0\left(\sqrt{iM}\right)}\right\}$$

$$+ \frac{{\rm Gr}+{\rm Gc}}{2Mi}\left\{\frac{\sqrt{-iM}K_1\left(\sqrt{-iM}\right)}{K_0\left(\sqrt{-iM}\right)} - \frac{\sqrt{iM}K_1\left(\sqrt{iM}\right)}{K_0\left(\sqrt{iM}\right)}\right\}, \tag{31}$$

$${\rm Nu}_{\rm s} = -\frac{S}{2iM}\left\{\frac{\sqrt{-iM}K_1\left(\sqrt{-iM}\right)}{K_0\left(\sqrt{-iM}\right)} - \frac{\sqrt{iM}K_1\left(\sqrt{iM}\right)}{K_0\left(\sqrt{iM}\right)}\right\}$$

$$+ \frac{S({\rm Gr}+{\rm Gc})}{2M^2}\left\{\frac{\sqrt{-iM}K_1\left(\sqrt{-iM}\right)}{K_0\left(\sqrt{-iM}\right)} + \frac{\sqrt{iM}K_1\left(\sqrt{iM}\right)}{K_0\left(\sqrt{iM}\right)}\right\}, \tag{32}$$

$${\rm Sh}_{\rm s} = -\frac{F}{2iM}\left\{\frac{\sqrt{-iM}K_1\left(\sqrt{-iM}\right)}{K_0\left(\sqrt{-iM}\right)} - \frac{\sqrt{iM}K_1\left(\sqrt{iM}\right)}{K_0\left(\sqrt{iM}\right)}\right\}$$

$$+ \frac{F({\rm Gr}+{\rm Gc})}{2M^2}\left\{\frac{\sqrt{-iM}K_1\left(\sqrt{-iM}\right)}{K_0\left(\sqrt{-iM}\right)} + \frac{\sqrt{iM}K_1\left(\sqrt{iM}\right)}{K_0\left(\sqrt{iM}\right)}\right\}. \tag{33}$$

It is to be noted that as $t \to \infty$, eqs (21)–(26) approach the results of steady-state expressions (28)–(33) respectively. Therefore, it can be concluded that the transient velocity, temperature, concentration, skin friction, Nusselt number and Sherwood number reach steady state for larger times. It is to be mentioned here that in the absence of mass transport (Gc = 0), the expressions for $U_{\rm s}$, $\theta_{\rm s}$, $\tau_{\rm s}$ and ${\rm Nu}_{\rm s}$ given by (28), (29), (31) and (32) coincide with the expressions for steady-state velocity as well as temperature, skin friction and Nusselt number in Deka and Paul [17].

5. Classical solutions ($S = 0$, $F = 0$)

Solutions derived in §3 for the fluid with thermal and mass stratifications are compared with the solutions of classical case, when there is no thermal and mass stratification. Here, the corresponding equations for the unstratified fluid ($S = 0$, $F = 0$) are non-dimensionalized by the same set of non-dimensional quantities (5) and the resulting non-dimensional equations for the classical case take the following forms:

$$\frac{\partial U_c}{\partial t} = \frac{\partial^2 U_c}{\partial R^2} + \frac{1}{R}\frac{\partial U_c}{\partial R} + \mathrm{Gr}\,\theta_c + \mathrm{Gc}\,\phi_c, \tag{34}$$

$$\frac{\partial \theta_c}{\partial t} = \frac{1}{\mathrm{Pr}}\left(\frac{\partial^2 \theta_c}{\partial R^2} + \frac{1}{R}\frac{\partial \theta_c}{\partial R}\right), \tag{35}$$

$$\frac{\partial \phi_c}{\partial t} = \frac{1}{\mathrm{Sc}}\left(\frac{\partial^2 \phi_c}{\partial R^2} + \frac{1}{R}\frac{\partial \phi_c}{\partial R}\right). \tag{36}$$

We solve eqs (34)–(36) by the Laplace transform technique, in the same way as referred earlier, subject to the initial and boundary conditions (9). We obtain the expressions of velocity (U_c), temperature (θ_c) and concentration (ϕ_c) profiles for the classical case as follows:

$$\begin{aligned} U_c = 1 + \frac{2}{\pi}\int_0^\infty \mathrm{e}^{-V^2 t}\Gamma(R, V)\frac{\mathrm{d}V}{V} \\ + \frac{\mathrm{Gr}+\mathrm{Gc}}{\pi}\int_0^\infty (1-\mathrm{e}^{-V^2 t})\Gamma_2(R,V)\frac{\mathrm{d}V}{V^2} \end{aligned} \tag{37}$$

$$\theta_c = 1 + \frac{2}{\pi}\int_0^\infty \mathrm{e}^{-V^2 t}\Gamma(R, V)\frac{\mathrm{d}V}{V} \tag{38}$$

and

$$\phi_c = 1 + \frac{2}{\pi}\int_0^\infty \mathrm{e}^{-V^2 t}\Gamma(R, V)\frac{\mathrm{d}V}{V}, \tag{39}$$

where

$$\begin{aligned} \Gamma_2(R, V) = R\frac{J_1(RV)\,Y_0(V) - Y_1(RV)\,J_0(V)}{J_0^2(V) + Y_0^2(V)} \\ + \frac{\{Y_1(V)\,J_0(RV) + Y_0(RV)\,J_1(V)\}\{J_0^2(V) - Y_0^2(V)\} - 2J_0(V)\,Y_0(V)\{J_1(V)\,J_0(RV) - Y_1(V)\,Y_0(RV)\}}{\{J_0^2(V) + Y_0^2(V)\}^2} \end{aligned} \tag{40}$$

and $\Gamma(R, V)$ is defined in eq. (27).

It is to be noted that when $S = 0$, eq. (22) assumes eq. (38) and similarly, when $F = 0$, eq. (23) assumes eq. (39).

The non-dimensional classical expressions of skin friction $\tau_c = -\left(\partial U_c/\partial R\right)|_{R=1}$, Nusselt number, $\mathrm{Nu}_c = -\left(\partial \theta_c/\partial R\right)|_{R=1}$ and Sherwood Number, $\mathrm{Sh}_c = -\left(\partial \phi_c/\partial R\right)|_{R=1}$ are derived from eqs (37)–(39) respectively as

$$\tau_c = \frac{2}{\pi}\int_0^\infty \mathrm{e}^{-V^2 t}\,\Gamma_1(V)\,\mathrm{d}V + \frac{\mathrm{Gr}+\mathrm{Gc}}{\pi}\int_0^\infty \left(1-\mathrm{e}^{-V^2 t}\right)\Gamma_3(V)\frac{\mathrm{d}V}{V^2}, \tag{41}$$

$$\mathrm{Nu}_c = \frac{2}{\pi}\int_0^\infty \mathrm{e}^{-V^2 t}\,\Gamma_1(V)\,\mathrm{d}V, \tag{42}$$

$$\mathrm{Sh}_c = \frac{2}{\pi}\int_0^\infty \mathrm{e}^{-V^2 t}\,\Gamma_1(V)\,\mathrm{d}V, \tag{43}$$

where

$$\begin{aligned}\Gamma_3(V) = &-\frac{2\left\{J_1(V)\,Y_0(V) - Y_1(V)\,J_0(V)\right\} + V\left\{J_0(V)\,Y_2(V) - Y_0(V)\,J_2(V)\right\}}{2\left\{J_0^2(V) + Y_0^2(V)\right\}} \\ &+ 2V\frac{J_1(V)\,Y_1(V)\left\{J_0^2(V) - Y_0^2(V)\right\} - Y_0(V)\,J_0(V)\left\{J_1^2(V) - Y_1^2(V)\right\}}{\left\{J_0^2(V) + Y_0^2(V)\right\}^2}\end{aligned}$$

and $\Gamma_1(V)$ is defined in eq. (27).

6. Results and discussion

In order to have a clear overview of the physical situation of the problem, numerical computations for velocity, perturbation temperature and concentration (hereafter called

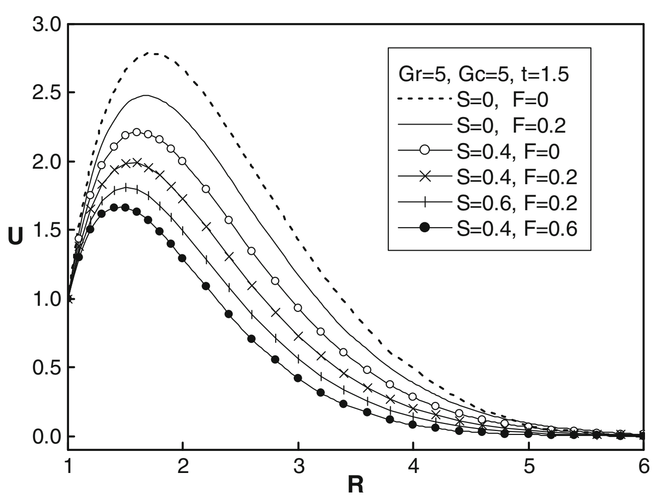

Figure 2. Effects of thermal and mass stratifications on velocity profile.

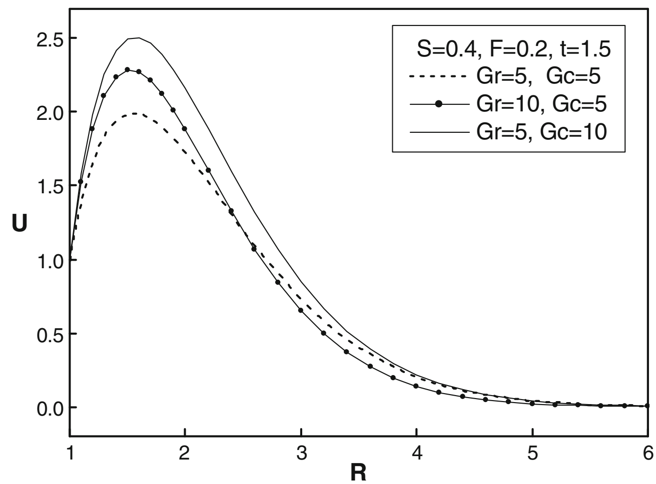

Figure 3. Effects of Gr and Gc on velocity profile.

temperature and concentration), skin friction, Nusselt number and Sherwood number are made for various physical parameters and presented in the figures. Solutions for the case of stratified fluid are compared with the classical case, when there is no thermal or mass stratification. It is observed that some expressions contain complex quantities and their conjugates. To overcome this, we have used in-built functions in MATHEMATICA to compute the numerical values. Furthermore, solutions of unsteady state for larger times are compared with the solutions of steady state.

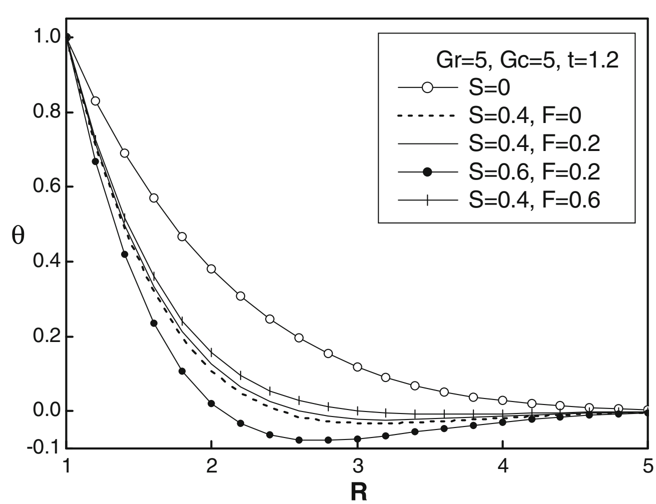

Figure 4. Effects of thermal and mass stratifications on temperature profile.

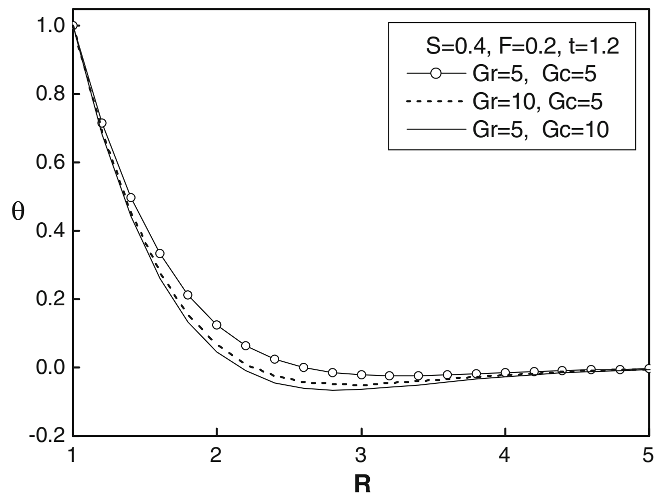

Figure 5. Effects of Gr and Gc on temperature profile.

Velocity profiles represented by figure 2 shows the effects of thermal stratification (S) and mass stratification (F) independently, keeping other parameters fixed (Gr $=5$, Gc $=5$), while figure 3 shows the effects of Gr and Gc for $S = 0.4$, $F = 0.2$. In figures 2 and 3, we have taken smaller time, $t = 1.5$, that corresponds to the time in the transient regime. It is observed that the mass stratification (keeping thermal stratification nill) reduces the velocity in the boundary layer. Likewise, it has been shown that the thermal stratification (keeping mass stratification nill) also reduces the velocity. The reduction in velocity is also due to the layering effect of thermal stratification, as it acts like a resistive force and this layering effect is more compared to the layering effect due to mass

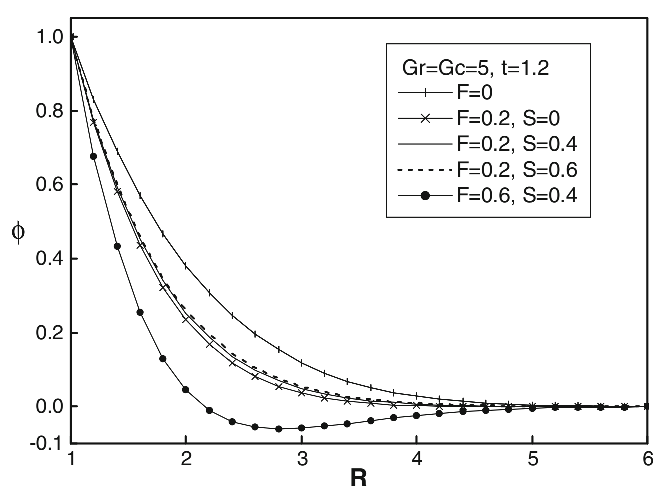

Figure 6. Effects of thermal and mass stratifications on concentration profile.

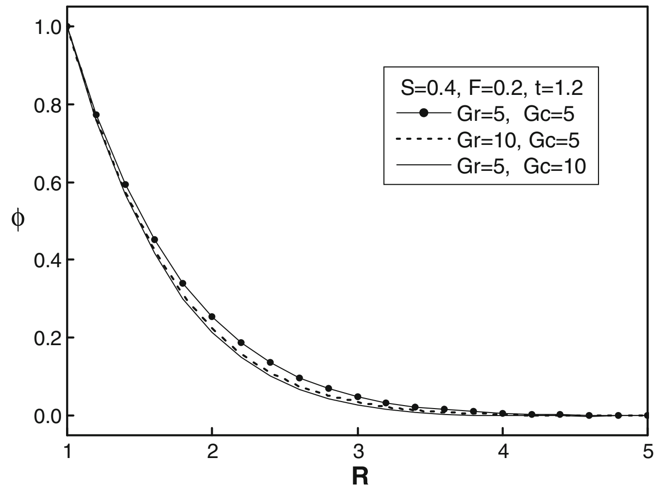

Figure 7. Effects of Gr and Gc on concentration profile.

stratification. For the simultaneous presence of the two stratifications, keeping mass stratification fixed, an increase in thermal stratification lowers the velocity; and keeping thermal stratification fixed, an increase in mass stratification lowers the velocity. It is further observed that an increase in Gr or Gc results in an increase in velocity because an increase in the values of thermal and mass Grashof number has the tendency to increase the thermal and mass buoyancy effects. Figure 4 reflects the effect of the two stratifications on fluid temperature, while figure 5 shows the effects of thermal and mass Grashof

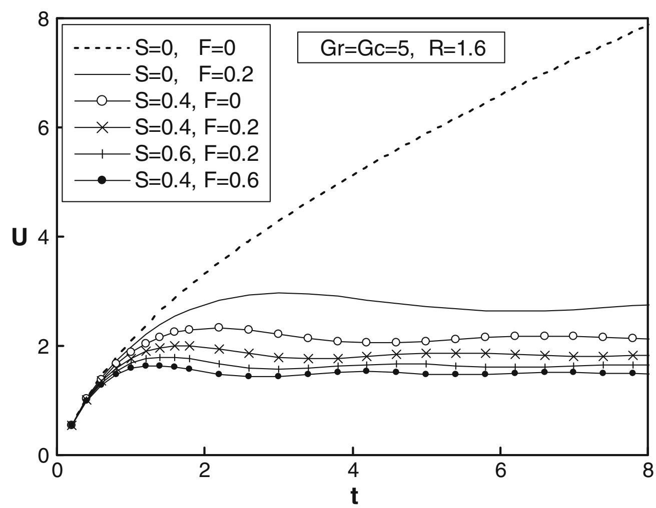

Figure 8. Effects of thermal and mass stratifications on velocity profile against time.

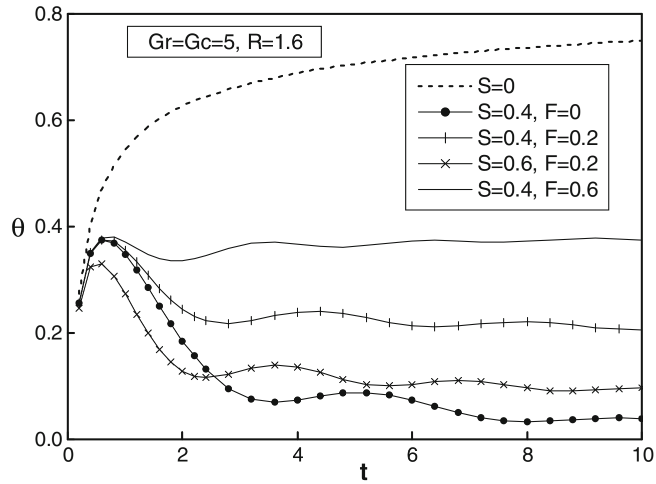

Figure 9. Effects of thermal and mass stratifications on temperature profile against time.

number. It is observed from figure 4 that with the increase in the thermal stratification and mass stratification parameters, the fluid temperature decreases and the decrease is more due to the thermal stratification. Another observation is that for strong thermal stratification, there is a reversal of flow, while the classical solution shows no reversal, as can be seen from figure 4. The flow reversal occurs because the cooler fluid from the bottom overshoots upward to a level, where the ambient temperature is higher. This type

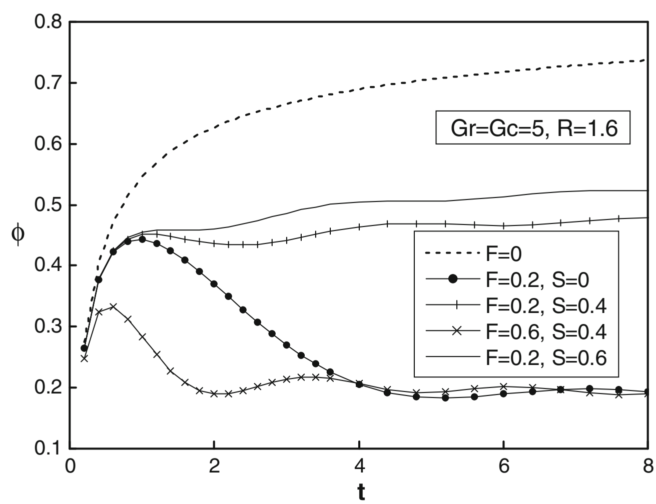

Figure 10. Effects of thermal and mass stratifications on concentration profile against time.

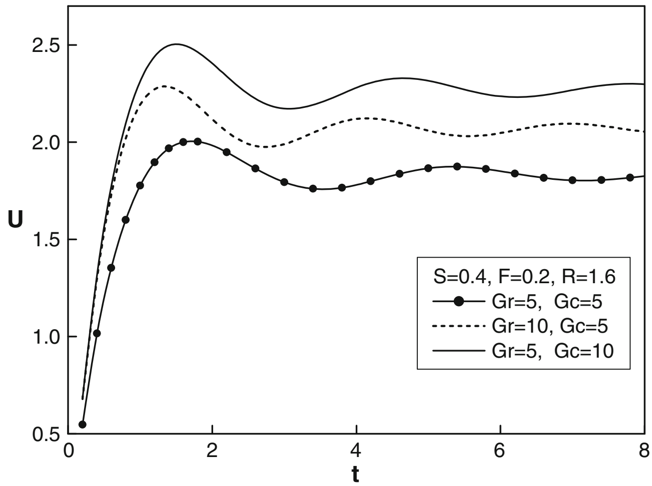

Figure 11. Effects of Gr and Gc on velocity profile against time.

of behaviour was predicted by earlier investigators (see Kulkarni *et al* [21], Deka and Paul [17]). The reduction of temperature with the increase in Gr or Gc shown in figure 5 is natural because the thermal and mass buoyancy forces assist the flow by increasing the fluid velocity (figure 3) and hence the heat is convected, thereby reducing the fluid temperature. The reduction in velocity and temperature with the thermal stratification was also observed by Loganathan and Ganesan [14] and Deka and Paul [17,18] in their numerical solution and analytical solution respectively. Likewise, the effects of the two stratifications on the species concentration shown in figures 6 and 7 are the same

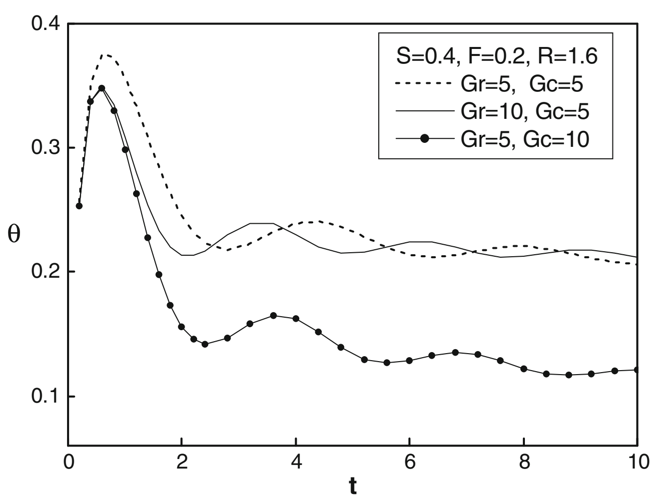

Figure 12. Effects of Gr and Gc on temperature profile against time.

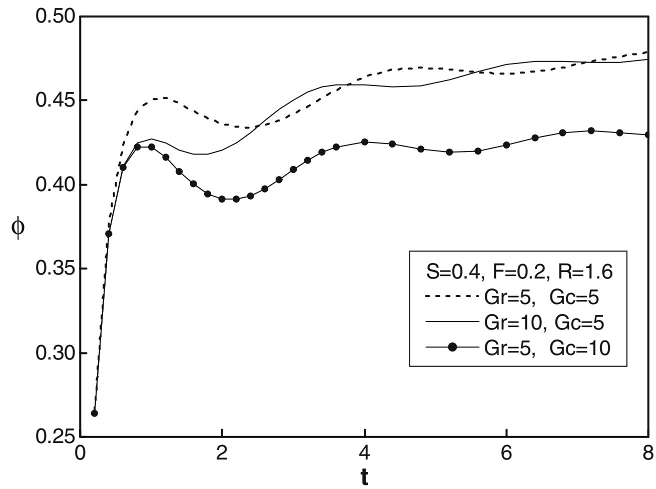

Figure 13. Effects of Gr and Gc on concentration profile against time.

as observed on temperature profiles. A decrease in velocity causes diffusion to dominate over convection caused by thermal as well as mass buoyancy forces. Hence, the concentration decreases due to the increase in thermal and mass stratification parameters. It has also been observed from figures 2, 4 and 6 that by applying thermal and mass stratifications, the velocity, temperature and concentrations are appreciably reduced compared to the classical ones ($S = 0$, $F = 0$), which is an added realism of the present study over the previous studies without stratifications.

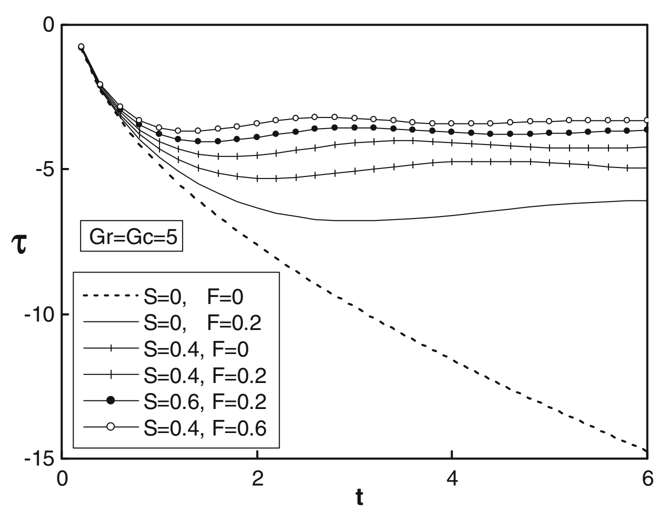

Figure 14. Effects of thermal and mass stratifications on skin friction.

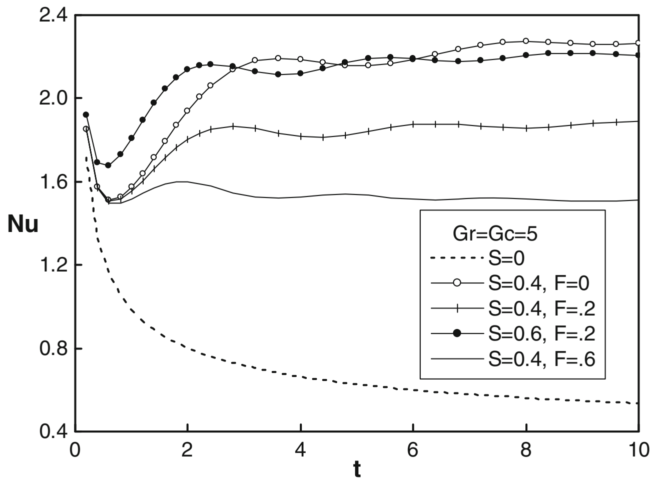

Figure 15. Effects of thermal and mass stratifications on Nusselt number.

The behaviour of the solutions at a fixed non-dimensional distance $R = 1.6$ (near the surface of the cylinder) is presented in figures 8, 9 and 10 to show the effects of the two stratifications on the fluid velocity, temperature and concentration against time. We have seen that there is a significant divergence between the classical and new solution. It is interesting to see that classical velocity, temperature and concentration increase unboundedly with time, but in the presence of stratifications considered, velocity, temperature and concentration reach steady state as time progresses. The simultaneous effects of the two stratifications lead to a faster approach to steady states as time progresses. On the contrary,

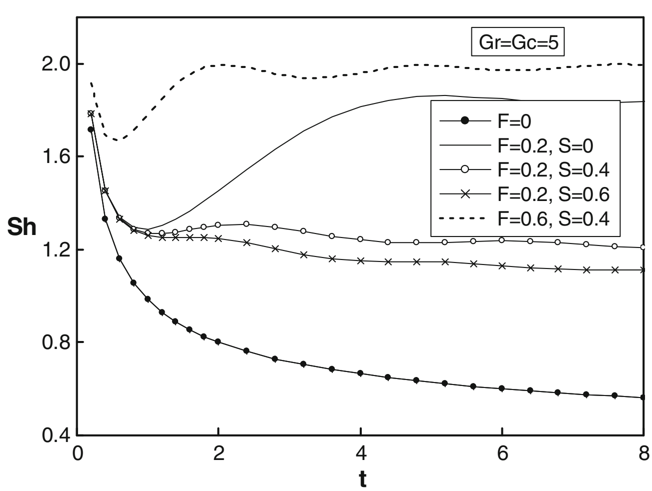

Figure 16. Effects of thermal and mass stratifications on Sherwood number.

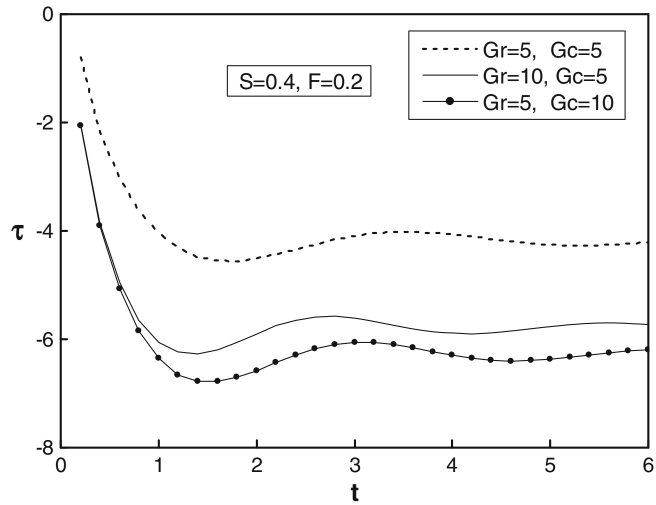

Figure 17. Effects of Gr and Gc on skin friction.

the thermal and mass Grashof numbers show no such role in converting the unsteady flow to a steady one as compared to the combined effect of the two stratifications appeared in figures 11, 12 and 13. Thus, we can conclude that the thermal stratification plays an important role in lowering the temperature and concentration near the plate as time progresses.

The behaviour of skin friction, rate of heat transfer (Nusselt number) and the rate of mass transfer (Sherwood number) against time are presented in figures 14, 15 and 16 for different values of thermal and mass stratification parameters including the classical case

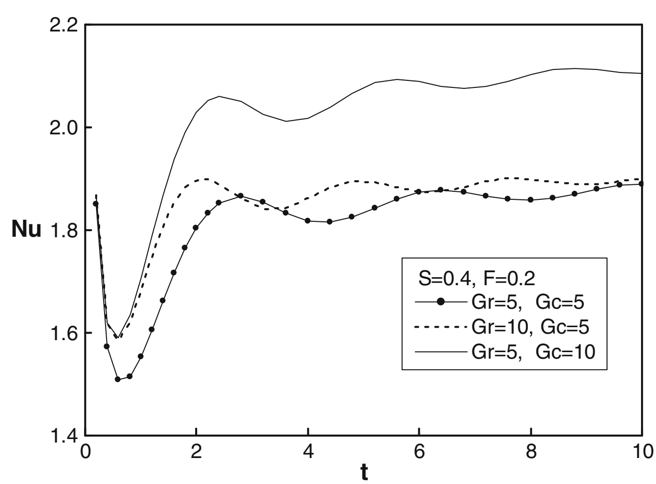

Figure 18. Effects of Gr and Gc on Nusselt number.

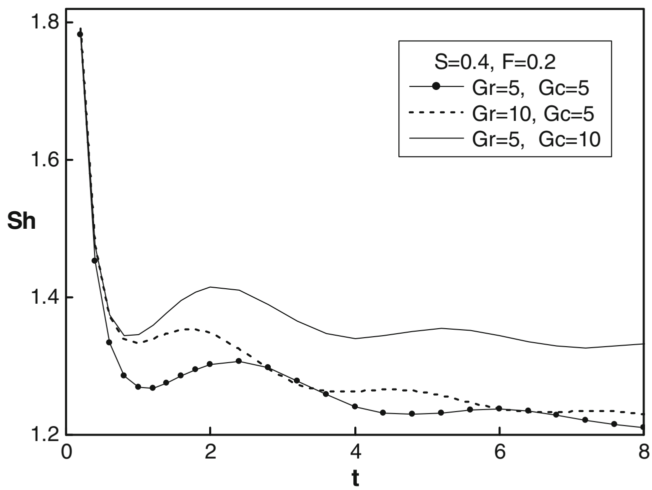

Figure 19. Effects of Gr and Gc on Sherwood number.

(when there is no thermal and mass stratification). It is observed that as time progresses, the skin friction, Nusselt number and Sherwood number approach a fixed value in the new solution (presence of thermal and mass stratification), while in the classical case these values decrease monotonically for all values of Gr and Gc. This is as expected, since the stratification transforms the transient state to a steady state as time progresses and so it can be concluded that the inclusion of stratification effect has an important role over the study without stratifications. On the other hand, an increase in Gc lowers the skin friction more as compared to Gr, while the reverse is true in case of Nusselt number and Sherwood number, which are displayed in figures 17, 18 and 19. This is also as expected, since the increase in velocity is more due to Gc than due to Gr (figure 3) and similar expectation is due to Nusselt and Sherwood number based on the behaviour of temperature (figure 5) and concentration (figure 7).

7. Summary

We have presented an analytical analysis for the transient natural heat and mass transfer from a moving heated vertical cylinder. Our analysis refines the thermodynamic energy and species concentration equation by introducing the thermal and mass stratifications which lead to a coupling effect among the temperature and concentration with the vertical velocity. The process thus considered, introduces a negative feedback mechanism and this mechanism results in a flow that approaches a steady state at large times. In contrast, in classical solutions, where there is no stratification, the disturbance caused by the moving cylinder continues and no steady state is reached. The steady state thus reached due to stratification also leads to a fixed constant value of Nusselt number, Sherwood number and skin friction as time progresses, while for classical solutions these values decrease monotonically. The effect of stratification also leads to a reversal of flow and this phenomenon may have application in the emergency cooling of the core of a nuclear reactor in the case of pump or power failure. Finally, the analytical solutions obtained by the Laplace transformation technique in terms of Bessel functions can be applied for validating numerical convection models.

Acknowledgement

One of the authors (R K Deka) acknowledges the support from the University Grants Commission, New Delhi, India.

Appendix

We have the Laplace transformation of U as

$$\bar{U} = \frac{1}{2}\left\{\frac{K_0(R\sqrt{p+iM})}{pK_0(\sqrt{p+iM})} + \frac{K_0(R\sqrt{p-iM})}{pK_0(\sqrt{p-iM})}\right\} - \frac{\mathrm{Gr}+\mathrm{Gc}}{2iM}\left\{\frac{K_0(R\sqrt{p+iM})}{pK_0(\sqrt{p+iM})} - \frac{K_0(R\sqrt{p-iM})}{pK_0(\sqrt{p-iM})}\right\}$$

which then can be expressed in terms of inverse Laplace transform as

$$U = \frac{1}{2}\left(1+\frac{\mathrm{Gr}+\mathrm{Gc}}{iM}\right)\mathrm{e}^{iM}I_1 + \frac{1}{2}\left(1-\frac{\mathrm{Gr}+\mathrm{Gc}}{iM}\right)\mathrm{e}^{-iM}I_2,$$

where

$$I_1 = L^{-1}\left\{\frac{K_0(R\sqrt{p})}{(p+iM)K_0(\sqrt{p})}\right\}$$

and

$$I_2 = L^{-1}\left\{\frac{K_0(R\sqrt{p})}{(p-iM)K_0(\sqrt{p})}\right\}.$$

Now, we apply complex inversion formula for determining I_1 and I_2 as follows:

$$I_1 = \frac{1}{2\pi i}\int_{\gamma'-i\infty}^{\gamma'+i\infty} \mathrm{e}^{pt}\frac{K_0(R\sqrt{p})}{(p+iM)K_0(\sqrt{p})}\mathrm{d}p = \sum \text{sum of residues},$$

where the integrand has a branch point at $p = 0$ and a simple pole at $p = -iM$.

Now $K_0(\sqrt{p})$ does not have zero at any point in the real and imaginary axes, if the branch cut is made along the negative real axis. To obtain I_1, we use the adjoining Bromwich contour (figure 20). Therefore, the line integral in I_1 may be replaced by the limit of the sum of the integrals over FE, ED, DC, CB and BA as $S_1 \to \infty$ and $S_0 \to 0$.

Here, the particular form of the contour integral has been chosen because the values along the paths DC, BA and FE approach zero as $S_1 \to \infty$ and $S_0 \to 0$.

Following Carslaw and Jaeger [20,22], along the paths CB and ED we choose, $p = V^2\mathrm{e}^{i\pi}$ and $p = V^2\mathrm{e}^{-i\pi}$, respectively.

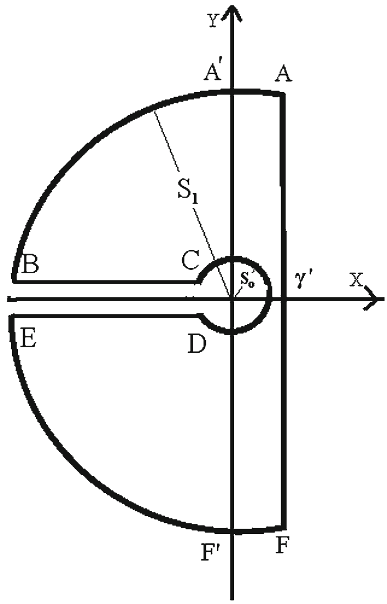

Figure 20. Bromwich contour of integration.

Therefore, on the path CB,

$$I_1 \text{ (along CB)} = \frac{1}{\pi i} \int_0^\infty \mathrm{e}^{-V^2 t} \frac{J_0(RV) - iY_0(RV)}{\left(V^2 - iM\right)\{J_0(V) - iY_0(V)\}} V \mathrm{d}V$$

and on the path ED,

$$I_1 \text{ (along ED)} = \frac{1}{\pi i} \int_0^\infty \mathrm{e}^{-V^2 t} \frac{J_0(RV) + iY_0(RV)}{\left(V^2 - iM\right)\{J_0(V) + iY_0(V)\}} V \mathrm{d}V.$$

Adding the above two integrals, we get

$$I_1 \text{ (along CB + ED)} = \frac{2}{\pi} \int_0^\infty \left\{ \frac{\mathrm{e}^{-V^2 t}}{V^2 - iM} \Gamma(R, V) V \right\} \mathrm{d}V,$$

where

$$\Gamma(R, V) = \frac{J_0(RV)Y_0(V) - Y_0(RV)J_0(V)}{J_0^2(V) + Y_0^2(V)}.$$

Also, the residue of the integrand I_1 at the pole $p = -iM$ is $= \mathrm{e}^{-iM}[K_0(R\sqrt{-iM})/K_0(\sqrt{-iM})]$.

Thus, from the theory of residues we have,

$$I_1 = \frac{2}{\pi} \int_0^{\infty} \left\{ \frac{e^{-V^2 t}}{V^2 - iM} \Gamma(R, V) V \right\} dV + e^{-iM} \frac{K_0\left(R\sqrt{-iM}\right)}{K_0\left(\sqrt{-iM}\right)}.$$

Similarly,

$$I_2 = \frac{2}{\pi} \int_0^{\infty} \left\{ \frac{e^{-V^2 t}}{V^2 + iM} \Gamma(R, V) V \right\} dV + e^{iM} \frac{K_0\left(R\sqrt{iM}\right)}{K_0\left(\sqrt{iM}\right)}.$$

Finally, we have,

$$\begin{aligned} U = & \frac{1}{2} \left\{ \frac{K_0\left(R\sqrt{-iM}\right)}{K_0\left(\sqrt{-iM}\right)} + \frac{K_0\left(R\sqrt{iM}\right)}{K_0\left(\sqrt{iM}\right)} \right\} \\ & + \frac{\mathrm{Gr} + \mathrm{Gc}}{2Mi} \left\{ \frac{K_0\left(R\sqrt{-iM}\right)}{K_0\left(\sqrt{-iM}\right)} - \frac{K_0\left(R\sqrt{iM}\right)}{K_0\left(\sqrt{iM}\right)} \right\} \\ & + \frac{2\,(\mathrm{Gr} + \mathrm{Gc})}{\pi M} \int_0^{\infty} \frac{e^{-V^2 t} \left\{ V^2 \sin(Mt) + M \cos(Mt) \right\}}{V^4 + M^2} \Gamma(R, V) V \, dV \\ & + \frac{2}{\pi} \int_0^{\infty} \frac{e^{-V^2 t} \left\{ V^2 \cos(Mt) - M \sin(Mt) \right\}}{V^4 + M^2} \Gamma(R, V) V \, dV. \end{aligned}$$

References

[1] E M Sparrow and J L Gregg, *Trans. ASME* **78**, 1823 (1956)
[2] R J Goldstein and D G Briggs, *Trans. ASME J. Heat Transfer* **86**, 490 (1964)
[3] G A Bottemanne, *Appl. Sci. Res.* **25**, 372 (1972)
[4] T S Chen and C F Yuh, *Int. J. Heat Mass Transfer* **23**, 451 (1980)
[5] J Heckel, T S Chen and B F Armaly, *Int. J. Heat Mass Transfer* **32**, 1431 (1989)
[6] R S R Gorla, *Int. J. Engg. Sci.* **27**, 77 (1989)
[7] K Velusamy and V K Garg, *Int. J. Heat Mass Transfer* **35**, 1293 (1992)
[8] P Ganesan and H P Rani, *Heat Mass Transfer* **33**, 449 (1998)
[9] P Ganesan and P Loganathan, *Acta Mech.* **150**, 179 (2001)
[10] P Ganesan and P Loganathan, *Heat Mass Transfer* **37**, 59 (2001)
[11] P Ganesan and P Loganathan, *J. Eng. Phys. Thermophys.* **75**, 899 (2002)
[12] H P Rani, *Heat Mass Transfer* **40**, 67 (2003)
[13] A Shapiro and E Fedorovich, *J. Fluid Mech.* **498**, 333 (2004)
[14] P Loganathan and P Ganesan, *J. Eng. Phys. Thermophys.* **79**, 73 (2006)
[15] H S Takhar, A J Chamkha and G Nath, *Heat Mass Transfer* **38**, 17 (2001)
[16] C Y Cheng, *Int. Comm. Heat and Mass Transfer* **36**, 351 (2009)
[17] R K Deka and A Paul, *Trans. ASME J. Heat Transfer* **134**, 042503-1 (2012)
[18] R K Deka and A Paul, *J. Mech. Sci. Technol.* **26(8)**, 2229 (2012)
[19] P K Kundu, *Fluid mechanics*, 3rd edn (Elsevier Academic Press, USA, 1990)
[20] H S Carslaw and J C Jaeger, *Operational methods in applied mathematics*, 2nd edn (Oxford Press, UK, 1948)
[21] A K Kulkarni, H R Jacobs and J J Hwang, *Int. J. Heat Mass Transfer* **30(4)**, 691 (1987)
[22] H S Carslaw and J C Jaeger, *Conduction of heat in solids*, 2nd edn (Oxford Press, UK, 1959)